Image-potential states on clean and hydrogen-covered Pd surfaces: Analysis of a one-dimensional model

Lenac, Z.; Šunjić, Marijan; Conrad, H.; Kordesch, M. E.

Source / Izvornik: **Physical review B: Condensed matter and materials physics, 1987, 36, 9500 - 9506**

Journal article, Published version
Rad u časopisu, Objavljena verzija rada (izdavačev PDF)

https://doi.org/10.1103/PhysRevB.36.9500

Permanent link / Trajna poveznica: https://urn.nsk.hr/urn:nbn:hr:217:669550

Image-potential states on clean and hydrogen-covered Pd surfaces: Analysis of a one-dimensional model

Z. Lenac
Pedagogical Faculty, YU-51000 Rijeka, Croatia, Yugoslavia

M. Šunjić
Department of Physics, University of Zagreb, P.O. Box 162, YU-41001 Zagreb, Croatia, Yugoslavia

H. Conrad and M. E. Kordesch
Fritz-Haber-Institut der Max-Planck-Gesellschaft, Faradayweg 4-6, D-1000 Berlin 33, Federal Republic of Germany

(Received 7 May 1987)

Theoretical calculations in a one-dimensional model give the energies of surface states on clean and hydrogen-covered Pd surfaces in very good agreement with those measured by high-resolution electron energy-loss spectroscopy and inverse photoemission experiments. Some general properties and the applicability of this class of one-dimensional models are discussed.

I. INTRODUCTION

The purpose of this paper is to analyze the underlying physics and the properties of the one-dimensional models used in the calculation of energies (and wave functions) of the surface states on metallic surfaces, and to apply them to specific cases of clean and H-covered Pd surfaces.

In Sec. II we describe the general shape of a well-known one-dimensional model potential[1-8] in order to compare the different choices of some essential parameters as used by various authors. In this context we discuss in Sec. III the possibility to determine the model parameters uniquely from the behavior of all surface states (crystal-induced and image-potential states), including their shifts upon hydrogen adsorption. We also derive a simple "scaling" rule reflecting an approximate invariance of the energies of higher image-potential states to the simultaneous change of the two parameters describing the surface layer.

We apply the model to the Pd(111) surface and get the results in good agreement with recent high-resolution electron energy-loss spectroscopy (HREELS) measurements[9,10] for a very reasonable set of parameters. The inverse photoemission (IP) results[11-13] are also discussed. Next, we study the changes induced upon adsorption of hydrogen,[9,10] the effect of which is included in the model by increasing the attractive part of the surface potential. Again the whole set of experimental results is reproduced by a shift of a single parameter by a reasonable amount. Moreover, the lowest-lying state which is located very close to the surface and appreciably influenced by the details of the bulk potential, disappears in this model, which is in agreement with the experimental observation. The Pd(100) surface is also briefly discussed, but with less success.

The critical discussion of the influence of all the model parameters on the energy of surface states is performed in Sec. IV for a well-known (111) surface of Cu. The conclusions are given in Sec. V.

II. THE MODEL

The most general version of the one-dimensional model potential that explains the existence of surface states on metallic surfaces[6-8] is divided into three regions, and is shown in Fig. 1. The bulk potential in the form

$$U(z)=-V_0+2V_G\cos(Gz+\alpha),\quad V_0,V_G>0,\ z<z_0 \tag{1}$$

is terminated at some point z_0. The origin $z=0$ will be fixed at the position of the last atomic layer, where we assume that $U(z)$ has a maximum value.[1,2] It gives $\alpha=0$ and $0<z_1<z_j$, where $z_j=a/2$ is the "jellium edge." $G=2\pi/a$ is the reciprocal-lattice vector and a is the (one-dimensional) direct lattice vector. The potential in the surface region $z_0<z<z_i$ is modeled by a constant potential U_0, which is an adjustable parameter, together with the "image-plane" position z_i:

$$U(z)=-U_0,\quad U_0>0,\ z_0<z<\begin{cases} z_i \\ z_i^* \end{cases}. \tag{2}$$

The second choice, z_i^*, in (2) corresponds to the case where U_0 is a potential constant all the way to its crossing with the image potential in the outside region (Fig. 1):

$$U(z)=-\frac{e^2}{4(z-z_i)}\ ,$$
$$z>\begin{cases} z_i, \textit{ classical} \text{ image potential} \\ z_i^*, \textit{ truncated} \text{ image potential} \end{cases}. \tag{3}$$

This general form of the potential has been specialized by different choices of boundaries in different papers.

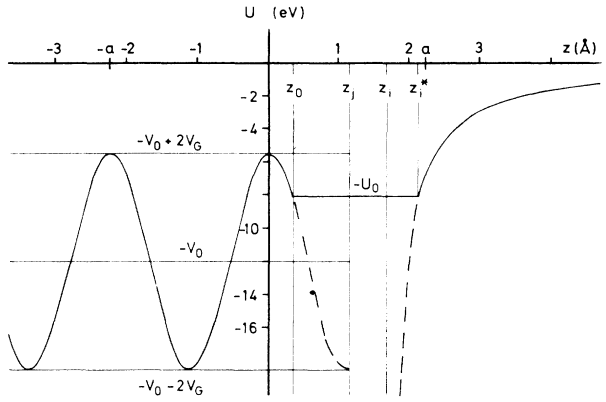

FIG. 1. The model potential. The bulk parameters (V_0, V_G, a) correspond to the L gap in Pd and the [111] direction. Note that the potential may generally have a discontinuity at z_0, depending on the parameters z_0 and U_0.

Smith,[6] for example, takes the classical image potential and sets $z_i = z_j$, i.e., the image plane is at the jellium edge. Then he makes two alternative choices: $z_0 = z_i$ or $z_0 = 0$, where the second choice gives better results. The potential in the surface region is equal to the average bulk potential: $U_0 = V_0$, so this model has no adjustable parameters.

Weinert *et al.*[7] take $z_0 = 0$, choose $U_0 = V_0 - 2V_G$ (top of the bulk potential), and extend U_0 to z_i^*, which is then treated as an adjustable parameter.

Ortuño and Echenique[8] choose $z_0 = a/2$, i.e., at the jellium edge, with the flat region $U_0 = V_0$ or $U_0 = V_0 + V_G$ extended to join the truncated potential at the point z_i^*. This point z_i^* (or equivalent z_i) is then varied to obtain agreement with experiments. In Sec. IV we shall discuss the crucial role of the z_0 parameter, showing that the wrong choice of z_0 cannot be corrected by any variation of U_0 or z_i.

In order to find the electronic wave functions and energies in one of these potentials, we shall use the phase accumulation method.[13,15] This method is equivalent to the wave-function matching in the case of the truncated potential.[7]

The electronic wave function in the vicinity of the high-symmetry points of the surface Brillouin zone[5,14–16] factorizes into

$$\Psi(\mathbf{r}) = e^{i\mathbf{K}\cdot\rho}\psi(z) .$$

The Schrödinger equation becomes

$$\left[-\frac{\hbar^2}{2m_\perp}\frac{d^2}{dz^2} + U(z)\right]\psi(z) = E\psi(z) ,$$

and the total energy is

$$E_{\text{tot}} = E + \frac{\hbar^2 K^2}{2m_\parallel} . \tag{4}$$

Here $\mathbf{K}$ is the wave-vector component along the surface, and $E < 0$ is the perpendicular energy of the bound electron states, i.e., surface states.

The solutions of the Schrödinger equation in the three regions are

$$\psi(z) = \begin{cases} C_3 e^{qz}\cos(pz+\delta), & z < z_0 \\ C_2\cos(\kappa z + \phi_0), & z_0 < z < z_i \text{ or } z_i^* \\ C_1 W_\nu(\rho), & z > z_i \text{ or } z_i^* . \end{cases} \tag{5}$$

Inside the solid $(z < z_0)$ we have taken the solution in the nearly-free-electron (NFE) approximation. The potential $U(z)$ opens the gap in the band structure at the Brillouin-zone edge where the wave vector k_z becomes complex:

$$k_z = p - iq, \quad p = \tfrac{1}{2}G, \; q > 0 .$$

We assume that $\mathbf{G}$ is along the surface normal. The parameters (q, δ) in the wave function (5) are determined from the relations

$$E_q = (4E_G\varepsilon + V_G^2)^{1/2} - (\varepsilon + E_G) , \tag{6a}$$

$$\tan(2\delta) = -\frac{\hbar^2}{m^*}pq/(\varepsilon - E_G + E_q) . \tag{6b}$$

Here $\varepsilon = E + V_0$ is the electron energy in the inner potential V_0, and

$$E_q = \frac{\hbar^2}{2m^*}q^2, \quad E_G = \frac{\hbar^2}{2m^*}p^2 .$$

The gap width is $2V_G$ and the center of the gap is at $E_G - V_0$. All energies are measured from the vacuum level $E_{\text{vac}} = 0$. If the top of the gap is above E_{vac}, as for the L gap in Pd(111), an infinite number of Rydberg states can exist near E_{vac}, contrary to the situation, e.g., for Cu(111), where the whole L gap is below E_{vac} and where only a part of Rydberg series can exist as sharp states.

The phase shift δ varies from $-\pi/2$ to 0 when E varies from the bottom to the top of the gap. The parameter q is equal to zero at both gap edges. Outside the gap we assume $q = 0$. The solutions can be found in that energy region as well, but in this one-dimensional model they propagate in the bulk without damping. Obviously, they are not true surface states[12] but in a proper calculation they turn out to be surface resonances.

In the *flat potential region* $(z_0 < z < z_i \text{ or } z_i^*)$ the wave vector κ is defined as

$$\kappa = \left[\frac{2m}{\hbar^2}(U_0 + E)\right]^{1/2} , \tag{7}$$

which gives the lowest possible value for E, i.e., $E > -U_0$.

In the *outside region* the wave functions are Whittaker functions, which are the solutions of

$$\left[\frac{d^2}{d\rho^2} + \frac{\nu}{\rho} - \frac{1}{4}\right]W_\nu(\rho) = 0 ,$$

where

$$\rho = (z - z_i)/(2a_0\nu), \quad a_0 = \hbar^2/me^2 ,$$

and we have defined

$$E=-\frac{1}{32}\frac{1}{\nu^2}\frac{e^2}{a_0},\quad \nu>0\ .$$

The lowest energy level ($\nu<1$) exists even if we replace the image potential by the step potential, and is usually called the crystal-induced or Shockley-inverted state. The higher-order levels exist due to the long (Coulombic) image-potential tail, and are called image-potential states.

The free-electron mass m has been replaced by $m_\perp$ and $m_\parallel$ for the electron motion perpendicular and parallel to the surface, respectively. We assume $m_\perp=m$ for $z>z_0$, but for $z<z_0$ we take $m_\perp=m^*$, where m^* represents the electron effective mass in the crystal. In this way we have, in the two-band (NFE) model, effectively taken into account the influence of other bands.

On the other hand, the energies of surface states disperse as a function of $\mathbf{K}$, described by the free-electron-like parabola (4) with the effective mass $m_\parallel$. However, for a given surface state, $m_\parallel$ depends upon the energy position of this state $E_{\rm tot}(K=0)=E$ in the gap.[16–19] For the theoretical discussion in the present paper, the parameter $m_\parallel$ is not important, but the direct comparison with experiment is possible only if the experimental energies are measured at $K=0$. If this is not the case, one has to use Eq. (4) to find E from $E_{\rm tot}$, and the knowledge of $m_\parallel$ becomes essential.

A. Phase accumulation model

In the flat potential region $z_0<z<z_i$ or z_i^*, the electronic wave function (5) can be represented in terms of the phase shifts ϕ_1 and ϕ_2 which correspond to the perfect electron reflection on the surface ($z=z_0$) and the image-potential barrier ($z=z_i$ or z_i^*), respectively:

$$\psi(z)=\begin{cases} A_1(e^{-i\kappa(z-z_0)}+e^{2i\phi_1}e^{i\kappa(z-z_0)}) \\ A_2(e^{i\kappa(z-z_i)}+e^{-2i\phi_2}e^{-i\kappa(z-z_i)})\ . \end{cases}$$

The bound states are given by the condition

$$\phi_2-\phi_1=\kappa(z_i-z_0)+m\pi,\quad m=0,1,2,\ldots\ , \tag{8}$$

where the first term on the right-hand side is the phase shift accumulated in the constant potential region.

The phases ϕ_1 and ϕ_2 have to be determined by matching the logarithmic derivatives of the wave functions at the boundaries, with the result

$$\kappa\tan\phi_1=-q+p\tan(\delta+pz_0)\ , \tag{9a}$$

$$\kappa\tan\phi_2=-\frac{d}{d\rho}\ln W_\nu(\rho)/(2a_0\nu)\,|_{\rho=\rho^*}\ , \tag{9b}$$

where

$$\rho^*=(z_i^*-z_i)/(2a_0\nu)\ .$$

The phase shift ϕ_2 for the classical image potential (matching at z_i) in the Wentzel-Kramers-Brillouin (WKB) approximation takes the simple form[5]

$$\phi_2=-\pi(\nu-\tfrac{1}{2})\ . \tag{10}$$

For fixed z_i,z_0, Eq. (8) give the discrete energy levels which are denoted uniquely by the quantum number $n=0,1,2,\ldots$.[7] The $n=0$ denotes the crystal-induced state, while $n=1,2,\ldots$ denotes the image-potential states. In the following we shall calculate the $\nu_n(z_i)$ dependence for the few lowest n values, using both the exact phase (9b) and the approximate WKB phase (10), with the following parameters: for the solid; G, E_B, V_G, and m^* ($V_0=E_G-V_G-E_B$), and for the surface region, U_0, z_0, and z_i ($z_i^*=z_i+e^2/4U_0$). Here E_B denotes the bottom of the energy gap.

III. DETERMINATION OF U_0 SENSITIVITY OF THE MODEL

We shall first discuss surfaces states on palladium surfaces. The energies of surface states are measured for the clean and H-covered Pd surfaces,[9–13] and we shall try to explain the observed energy shifts.

A. Clean Pd(111) surface

The $L_2'L_1$ gap in bulk Pd is opened by the $\mathbf{G}$ vector perpendicular to the (111) plane of the solid. It occurs at $\bar\Gamma$ on Pd(111), so in this respect the one-dimensional model is justified. The parameters appropriate for the [111] direction in Pd are $a=2.24$ Å, $G=2.80$ Å^{-1}, $E_G=7.48(m/m^*)$ eV. The parameters for the Pd L gap are[20–22] $V_G=3.3$ eV and $E_B=-4.6$ eV. Fitting the dispersion curve for the ΓL direction[20] to a free-electron-like parabola (NFE model), we obtain $m^*/m=0.7$, which gives $E_G=10.7$ eV and $V_0=12.0$ eV.

In the truncated image-potential model, for the parameters $z_0=0$, $U_0=5.5$ eV, and $z_i=2.1$ Å, we obtain in a set of eigenenergies [Fig. 2(a), Table I]

$$E=-3.7,\ -0.72,\ -0.22,\ -0.096\ \text{eV}$$

TABLE I. Calculated and measured energies of surface states on Pd(111) (all values in eV).

State n	Crystal induced	$n=1$	$n=2$	$n=3$
$U_0=5.4$ eV, $z_i=2.1$ Å	−3.7	−0.72	−0.22	−0.096
$U_0'=9.0$ eV, $z_i=z_i'=1.5$ Å	−4.9	−0.76	−0.22	−0.096
HREELS	−6.1	−0.75	−0.25	
Inverse PE[a]	−4.3	−0.56		
$U_0=9$ eV, $z_i=2.1$ Å	−6.0	−1.4	−0.33	−0.13
$U_0'=15$ eV, $z_i=1.5$ Å	−9.1	−1.5	−0.33	−0.13
HREELS Pd(111)/H	below bottom of gap	−1.25	−0.33	

[a]Reference 13.

in very good agreement with HREELS results for the first and second states of Pd(111):[9,10]

$$E=-0.75,\ -0.25\ \text{eV}\ . \tag{11}$$

Figure 2(a) also shows the curves $v(z_i)$ for the classical image potential, with the approximation (10). The two procedures do not differ very much except for the lowest state, which is strongly localized in the region between z_i and z_0 in the classical case. Figure 2(b) gives the same results in terms of binding energies versus z_i.

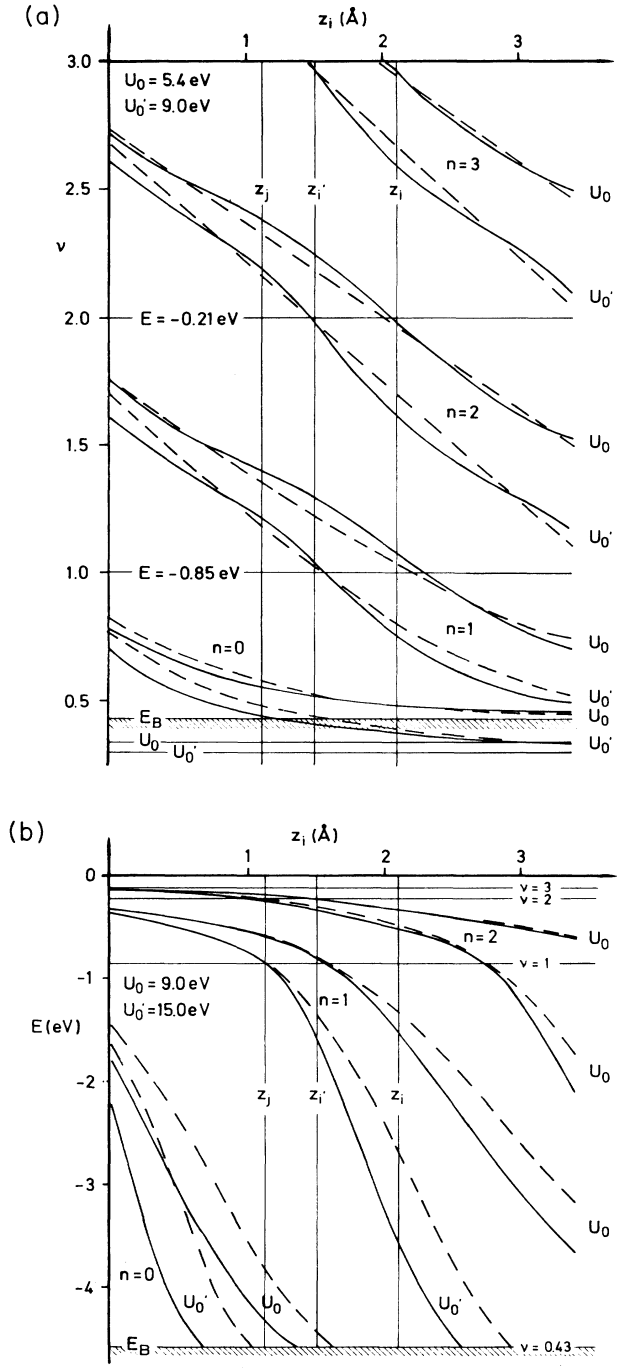

FIG. 2. $v(z_i)$ curves (a) and $E(z_i)$ curves (b) for Pd(111) crystal-induced and image-potential states. The truncated (solid lines) and classical image (dashed lines) solutions are given for two U_0 values, with $z_0=0$. Denoted are the values of the parameters z_i and z_i' that we have chosen to explain the experimental values.

The choice of U_0 is obviously not unique. It would be equally physically justified to choose any value of $-U_0$ in the range between $-V_0+2V_G=-5.4$ eV and $-V_0-2V_G=-18.6$, so one may want to discuss the consequences of these possible choices. For instance, taking $-U_0'=-9.0$ eV and shifting z_i to $z_i'=1.5$ Å gives the sequence of energy levels

$$E=-4.9,\ -0.76,\ -0.22,\ -0.096\ \text{eV}\ .$$

There is a noticeable difference only for the lowest level, which could therefore serve to determine the proper value of U_0. However, since the experiments give the energy of this level close to the bottom of the gap,[9,13] its dispersion may become a separate question. For the other levels, we notice the "scaling" connection between the optimal values for the parameters U_0, z_i and U_0, z_i':

$$z_i' \approx \left[\frac{U_0}{U_0'}\right]^{1/2} z_i\ . \tag{12}$$

This simple rule is valid for energies $|E| \ll U_0$, and is derived in the Appendix.

Figure 2(a) shows indeed that the curves $v(z_i)$ for $U_0=5.4$ and 9.0 eV are approximately parallel (*uniformly shifted*) for $|E| \ll U_0$. In other words, for each U_0 we can find a corresponding z_i which gives a good sequence of energy levels.

For $E \to -U_0$ the curves bend, which leads to strong differences in the lowest-level energies for different U_0.

The energy levels (11) are obtained by extrapolating the HREELS data from $\bar{M}$ to $\bar{\Gamma}$ with $m_\parallel = m$. This procedure is expected to be correct for the image-potential states, but gives $E=-6.1$ eV for the crystal-induced state.[9]

The IP data for Pd(111) are somewhat different: the two lowest surface states (measured close to $\bar{\Gamma}$) are[13]

$$E=-4.3,\ -0.56\ \text{eV}\ . \tag{13}$$

We can reproduce those data exactly if we take $z_i = a/2 = 1.1$ Å (with $U_0=9.0$ eV). Let us notice that in Ref. 13 $m_\perp = m$ was assumed, which put the maximum $(-V_0+2V_G)$ of the bulk potential very close, 2 eV below the vacuum level. Therefore only a large shift of U_0 from V_0-2V_G gives the correct energies (13).

If we require that the HREELS data (at $\bar{M}$) correspond to the IP data (at $\bar{\Gamma}$), we must take $m_\parallel = 0.73m$ for the crystal-induced state and $m_\parallel = 0.97$ for the (first) image-potential state. While for the image-potential states $m_\parallel = m$ is consistent with both HREELS and IP data, the IP measurements give a rather low value $m_\parallel = 0.35m$ for the crystal-induced state.[13]

1. *Electronic wave functions*

Figures 3(a) and 3(b) show the electronic wave functions (5) of the three lowest states, calculated with the

parameters $U_0=5.4$ eV, $z_i=2.1$ Å and $U_0=9.0$ eV, $z_i=1.5$ Å, respectively. In both cases the results are very similar, with the deviation for the lowest state, which is visible also in the eigenenergies, as discussed before. Particularly, the $n=0$ state is shown as a surface state ($E>E_B$) in Fig. 3(a), and as a surface resonance ($E<E_B$) in Fig. 3(b) as discussed before.

In Fig. 3 the wave functions are not normalized: we have taken the Whittaker-function coefficient $C_1=1$, and the other two coefficients are

$$C_2=W_\nu(\rho^*)/\cos\phi_2 ,$$

$$C_3=C_2\cos\phi_1/[e^{qz_0}\cos(pz_0+\delta)] .$$

B. Adsorption of hydrogen

Hydrogen is adsorbed somewhere in the region $0<z<z_i$, so we expect it to lead to the following modification of the effective potential.

(1) The bulk potential (V_0, V_G) does not change for $z<0$.

(2) The vacuum potential ($z>z_i$) does not change—the image-plane position stays as for the clean surface, and we neglect the influence of the small work-function change on the value of the inner potential V_0.

(3) The effect of adsorbed hydrogen is expected to lead to a more attractive potential in the surface region $0<z<z_i$. This increase of V_0 will be shown to lead to the changes in the image-state energies, as was observed experimentally.[9,10]

The shift $U_0\rightarrow U_0'$ (with z_i fixed) is connected with the energy shift $E\rightarrow E'$, i.e., $\nu\rightarrow\nu'$, through a simple relation

$$(U_0')^{1/2}-(U_0)^{1/2}=6.13\frac{(\nu-\nu')}{z_i\ (\text{Å})}\ (\text{eV}^{1/2}) . \tag{14}$$

The derivation is given in the Appendix, assuming $|E'|\ll U_0'$.

A certain shift $\Delta U_0=U_0'-U_0$ leads to a uniform downward shift $\Delta\nu$ of *all* image-potential states. The energies are also *lowered*, but the lowest (crystal-induced) state is shifted most. If its energy was close to the bottom of the gap on the clean surface, H adsorption may push it below and it may vanish—as is indeed the case with Pd. Let us notice that the crystal-induced state usually does not satisfy the condition $|E'|\ll U_0'$, and therefore its energy shift will not obey Eq. (14) closely.

Experimentally observed energies of image-potential states for Pd(111)/H are[9,10]

$$E'=-1.25,\ -0.33\ \text{eV} .$$

The shifts for Pd(111)→Pd/H are $\nu-\nu'=0.24$ for both $n=2$ and $n=3$ states, so for a given U_0 from Eq. (14) we can calculate U_0' and test the validity of the model. Let us do that with the two sets of parameters:

(a) $U_0=5.4$ eV$\rightarrow U_0'=9.0$ eV, $z_i=2.1$ Å

or

(b) $U_0=9.0$ eV$\rightarrow U_0'=15.0$ eV, $z_i=1.5$ Å .

The resulting electronic energies are

(a) $E'=-6.0,\ -1.4,\ -0.33$, and -0.13 eV ,

(b) $E'=-9.1,\ -1.5,\ -0.33$, and -0.13 eV .

Again the difference is seen only in the lowest-energy state, which is now, in both cases, deep below the bottom of the gap.

Figure 2(a) shows the ν and ν' values for Pd(111) and Pd(111)/H with the (a) parameters, while Fig. 2(b) shows the E and E' values for Pd(111) and Pd(111)/H with the (b) parameters.

Figure 3(c) shows the wave functions calculated with the shifted (a) parameters $U_0'=9.0$ eV, $z_i=2.1$ Å; it is clearly seen that the image-potential states on Pd/H are more localized near the surface than on clean Pd [Fig. 3(a)], while the $n=0$ surface state becomes the $n=0$ surface resonance.

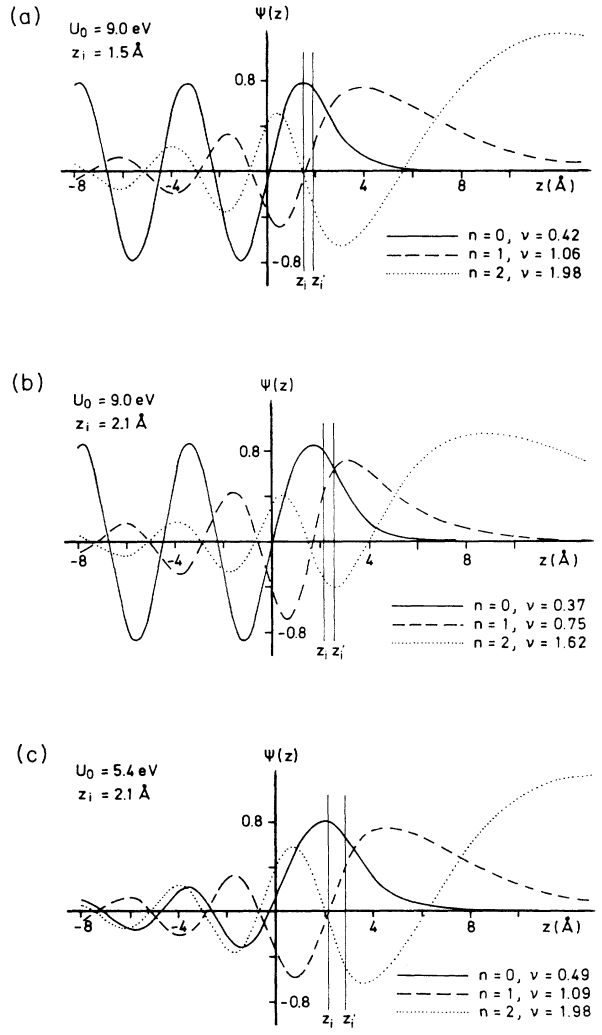

FIG. 3. The wave functions of the three lowest surface states on Pd(111) surface. We take $z_0=0$ for all curves.

C. Pd(100) surface

Experimental values for the clean Pd(100) surface are[10] $E=-0.95$, -0.19 eV, which corresponds to $\nu=0.95$, 2.1. These results are not far from the Rydberg series $\nu=1,2,3,\ldots$, and could be reproduced easily for any reasonable model potential (1).

Experimental values for Pd(100)/H are[10] $E'=-2.0$, -0.72, -0.22 eV, i.e., $\nu'=0.65$, 1.1, 1.9.

If we assume that the first excited surface state is shifted due to H adsorption, we obtain $\Delta\nu=2.1-1.1=1.0$, which is a large shift. Namely, the equation (14) can be satisfied for large $\Delta\nu$ either with small U_0 or with large z_i.

The two lowest levels $\nu'=0.65$ and 1.1 are very close, which can be reproduced if the lowest-level curve $\nu'(z_i)$ is strongly bent [Fig. 2(a)]. For the lowest level this gives $|E'|\approx U_0'$ and therefore $U_0'\lesssim 4$ eV. This in turn implies that $U_0\lesssim 2$ eV, which is a rather strong assumption.

In other words, the experimental results for Pd(100) and Pd(100)/H surface states can be reproduced in the present model, but with a rather unlikely choice of parameters (U_0,U_0'). At this point we should stress the following.

(i) The surface-state energies for Pd(100) and Pd(100)/H are obtained by extrapolating the HREELS experimental data[10] from $\bar{X}$ to $\bar{\Gamma}$ with $m_{\parallel}=m$, which might not be correct (especially for the crystal-induced state).

(ii) The validity of the one-dimensional model is rather questionable for the Pd(100) surface, since the projected Pd bulk band structure onto $\bar{\Gamma}$-$\bar{X}$ direction in the second Brillouin zone (where the experimental values of **K** fall) has not been calculated. Therefore we cannot analyze the width and the position of the gap and its dispersion which are the essential criteria for the validity of the one-dimensional model.

IV. ANALYSIS OF z_0 SENSITIVITY OF THE MODEL

Up to this point we have demonstrated, using the Pd(111) surface as an example, the influence of the model parameters U_0 and z_i on the energies of the surface states. The parameter z_0 which describes the bulk edge remains constant ($z_0=0$). However, in principle we could take a realistic value for z_0 anywhere in the interval $0<z_0<z_j=a/2$, so, in general, in the present model, the energy of a surface state is a function of three parameters (U_0, z_0, z_i). On the other hand, only the two lowest states are sensitive to the particular choice of these "surface" parameters, since their wave functions are localized close to the surface (Fig. 3). The wave functions of the higher states have their maxima in the classical imagelike tail of the potential, and therefore their energies follow closely the Rydberg series, independent of U_0, z_0, z_i.

To discuss more precisely the influence of all "surface" parameters we must find a case where the energies of two lowest surface states have been determined at $\bar{\Gamma}$, as in the case with the Cu(111) surface. The measured energies are $E_0=-5.33$ eV and $E_1=-0.90$ eV.[23–25] In principle, these energies are functions of three parameters:

$$E_0=E_0(z_0,U_0,z_i)\ ,$$

$$E_1=E_1(z_0,U_0,z_i)\ .$$

Taking E_0 and E_1 from experiments, we can determine two of the parameters:

$$U_0=U_0(z_0,E_0,E_1)\ ,$$

$$z_i=z_i(z_0,E_0,E_1)$$

as functions of the bulk edge position z_0. The actual calculation is done iteratively, and the curves $U_0(z_0)$ and $z_i(z_0)$ are shown in Fig. 4. It explains, e.g., the difficulties of Ortuño and Echenique,[8] who took $z_0=0.5a$, and therefore could not find a z_i value that gives exactly both E_0, E_1 values, neither with $U_0=V_0$ nor with $U_0=V_0-V_G$. Similarly, Weinert *et al.*[7] chose $z_0=0$, but with $U_0=V_0-2V_G$ they also could not obtain exact E_0, E_1 values.

The most interesting feature on Fig. 4 is the *constant* value of z_i for all calculated z_0 values. This means that the present model indicates the value of $z_i=1.27$ Å for the Cu(111) surface, regardless of z_0 and U_0. It places the image plane 0.2 Å outside the jellium edge, which is quite a reasonable result.[26,27]

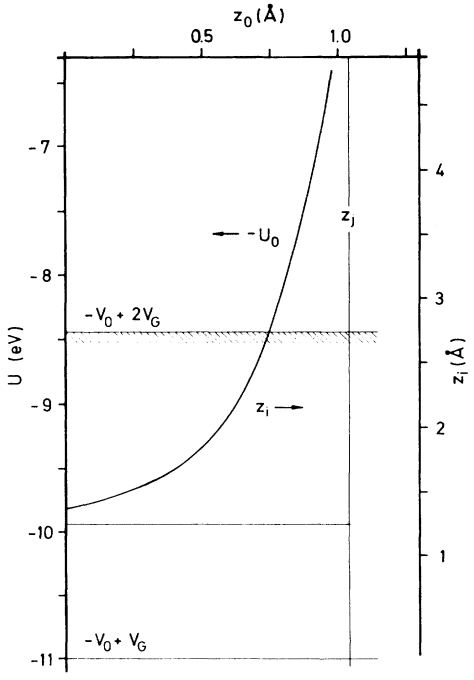

FIG. 4. $U_0(z_0)$ and $z_i(z_0)$ curves that fit the two surface states in the L gap of Cu. The bulk parameters are (Ref. 6) $V_0=13.54$ eV, $V_G=2.55$ eV, $a=2.08$ Å.

V. CONCLUSIONS

In this paper we have analyzed some properties of the one-dimensional matching models of the crystal-induced and image-potential states on clean and hydrogen-covered transition-metal surfaces. In particular, we have applied it successfully to the Pd(111) surface where all the states were described by a single choice of parameters. The hydrogen adsorption was assumed to lead to an increase of the attractive U_0 potential, and a reasonable shift of U_0 again provided good agreement with experimentally observed energies. This model also qualitatively explained the disappearance of the lowest state, which was, upon H adsorption, pushed far below the gap. A new H-induced (and dispersionless) state appears and is experimentally observed,[9,10] but its analysis is outside the framework of the present theory.

For the Pd(100) surface we do not have all the necessary input parameters of the band structure to perform the relevant calculations, but our analysis shows that a one-dimensional model might not be adequate.

Our analysis explicitly demonstrates the "scaling" properties of the model, i.e., the experimental data for energies of image-potential states can be explained by different choices of U_0, z_i, z_0 values. Usually, z_0 is taken as a fixed parameter,[6-8] but it seems physically more reasonable to vary the local surface-sensitive quantity z_0 than the image-plane position z_i, which essentially reflects a property of the bulk metallic electrons. Although the one-dimensional model might appear too crude to predict the position of z_i, in the case of the Cu(111) surface we have found that $z_i = 1.27$ Å yields reasonable results, independent of the set of z_0, U_0 parameters chosen to fit both the crystal-induced and image-potential surface states.

ACKNOWLEDGMENT

This work was partially supported by the U.S.–Yugoslav Joint Board on Scientific and Technological Cooperation, Grant No. JFP-695/NBS.

APPENDIX

We shall derive two simple and useful rules (12) and (14), starting from the phase matching rule (8). For $(U_0, z_i, \nu) \rightarrow (U_0', z_i', \nu')$, we obtain $\phi_2' - \phi_1' = \kappa' z_i' + n\pi$. The phase change $\phi_2' - \phi_2$ is much greater than the phase change $\phi_1' - \phi_1$,[6] so the total phase change is approximately given by

$$\Delta\phi \approx \phi_2' - \phi_2 \approx \pi(\nu - \nu') \approx \kappa' z_i' - \kappa z_i \ . \tag{A1}$$

Here we have also used the WKB approximation (10) for $\Delta\phi_2$, since we have shown that it reproduces reasonably well the truncated curves $\nu(z_i)$ [Fig. 2(a)].

(i) Let us assume that the energies remain constant: $\nu = \nu'$. From (A1)

$$\kappa' z_i' \approx \kappa z_i, \quad \nu = \nu' \ . \tag{A2}$$

Except eventually for the lowest surface state, we can assume

$$|E'| \ll U_0' \tag{A3}$$

and approximate $\kappa \approx (2mU_0/\hbar^2)^{1/2}$, $\kappa' \approx (2mU_0'/\hbar^2)^{1/2}$, which inserted into Eq. (A2) immediately leads to Eq. (12).

(ii) Let us assume that the image plane is not shifted: $z_i = z_i'$. With the assumption (A3) we find from Eq. (A1)

$$(U_0')^{1/2} - (U_0)^{1/2} = \frac{\pi}{\sqrt{2}} \frac{(\nu - \nu')}{(z_i - z_0)} (e^2 a_0)^{1/2} \ ,$$

which leads to Eq. (14).

[1] E. T. Goodwin, Proc. Cambridge Philos. Soc. **35**, 205 (1939).
[2] F. Forstmann, Z. Phys. **235**, 69 (1970).
[3] M. Kolar and I. Bartos, Czech. J. Phys. B **23**, 179 (1973); P. M. Echenique and J. B. Pendry, J. Phys. C **11**, 2065 (1978).
[4] J. B. Pendry and S. J. Gurman, Surf. Sci. **49**, 87 (1975).
[5] E. G. McRae, Rev. Mod. Phys. **51**, 541 (1979).
[6] N. V. Smith, Phys. Rev. B **32**, 3549 (1985).
[7] M. Weinert, S. L. Hulbert, and P. D. Johnson, Phys. Rev. Lett. **55**, 2055 (1985).
[8] M. Ortuño and P. M. Echenique, Phys. Rev. B **34**, 5199 (1986).
[9] H. Conrad, M. E. Kordesch, R. Scala, and W. Stenzel, J. Electron. Spectrosc. Relat. Phenom. **38**, 289 (1986).
[10] H. Conrad, M. E. Kordesch, W. Stenzel, M. Sŭnjić, and B. Trninić-Radja, Surf. Sci. **178**, 578 (1986).
[11] P. D. Johnson and N. V. Smith, Phys. Rev. Lett. **49**, 290 (1982).
[12] D. A. Wesner, P. D. Johnson, and N. V. Smith, Phys. Rev. B **30**, 503 (1984).
[13] S. L. Hulbert, P. D. Johnson, and M. Weinert, Phys. Rev. B **34**, 3670 (1986).
[14] R. A. Bartynski, T. Gustaffson, and P. Soven, Phys. Rev. B **31**, 4745 (1985).
[15] V. Dose, Surf. Sci. Rep. **5**, 337 (1985).
[16] N. V. Smith, and D. P. Woodruff, Prog. Surf. Sci. **21**, 295 (1986).
[17] J. B. Pendry, C. G. Larsson, and P. M. Echenique, Surf. Sci. **166**, 57 (1986).
[18] P. M. Echenique and J. P. Pendry, Surf. Sci. **166**, 69 (1986).
[19] K. Giesen, F. Hage, F. J. Himpsel, H. J. Ries, W. Steinmann, and N. V. Smith, Phys. Rev. B **35**, 975 (1987).
[20] N. E. Christensen, Phys. Rev. B **14**, 3446 (1976).
[21] F. J. Himpsel and D. E. Eastman, Phys. Rev. B **18**, 5236 (1978).
[22] S. G. Louie, Phys. Rev. Lett. **40**, 1525 (1978).
[23] S. D. Kevan, Phys. Rev. Lett. **50**, 526 (1983).
[24] S. L. Hulbert, P. D. Johnson, N. G. Stoffel, W. A. Royer, and N. V. Smith, Phys. Rev. B **31**, 6815 (1985).
[25] K. Giesen, F. Hage, F. J. Himpsel, J. H. Ries, and W. Steinmann, Phys. Rev. B. **33**, 5241 (1986).
[26] N. D. Lang and W. Kohn, Phys. Rev. B **7**, 3541 (1973).
[27] S. Ossicini, M. Bertoni, and P. Gies, Europhys. Lett. **1**, 661 (1986).